Development of Potent and Selective Phosphinic Peptide Inhibitors of Angiotensin-Converting Enzyme 2

Andreas Mores,[†] Magdalini Matziari,[†] Fabrice Beau,[‡] Philippe Cuniasse,[‡] Athanasios Yiotakis,[†] and Vincent Dive*[,‡]

Department of Chemistry, Laboratory of Organic Chemistry, University of Athens, Panepistimiopolis Zografou 15771, Athens, Greece, and CEA, DSV, Service d'Ingénierie Moléculaire des Protéines (SIMOPRO), Bat 152, CE-Saclay, Gif/Yvette Cedex 91191 France

Received October 10, 2007

Angiotensin-converting enzyme 2 (ACE2), a recently identified human homologue of angiotensin-converting enzyme, is a zinc metallocarboxypeptidase which may play a unique role in cardiovascular and renal function. Here we report the discovery of potent and selective inhibitors of ACE2, which have been identified by evaluating a series of phosphinic di- and tripeptides of the general formula: Z-Xaa(PO_2-CH_2)YaaOH and Ac-Zaa-Xaa(PO_2-CH_2)YaaOH. The most potent inhibitor in this series is a tripeptide that displays a K_i value of 0.4 nM toward ACE2 and is 3 orders of magnitude less potent toward carboxypeptidase A. Phosphinic tripeptides exhibit high potency exclusively when the Xaa position is occupied by a pseudoproline. A model of interaction between one inhibitor of this series and ACE2 suggests that the critical role played by a proline in inhibitors, but also for substrates hydrolysis, may rely on the presence of Tyr^{510} in the ACE2 active site.

Introduction

Angiotensin-converting enzyme (ACE[a]), a zinc dipeptidyl carboxypeptidase, is a key enzyme in the renin-angiotensin system (RAS), which cleaves the inactive angiotensin I decapeptide into the potent vasoconstrictor angiotensin II octapeptide and inactivates the vasodilator bradykinin.[1,2] Over the last two decades, inhibitors of ACE have emerged as first-line therapy for a range of cardiovascular and renal diseases, including hypertension, congestive heart failure, myocardial infarction, and diabetic nephropathy.[3,4] Recently, the classic view of the RAS has been challenged by the discovery of ACE2, the first known human homologue of ACE.[5,6] ACE2 has significant sequence similarity to ACE, but also displays several key functional differences: it contains a single zinc active site, it functions as a carboxypeptidase, and is not affected by classic ACE inhibitors. Based on the study of a panel of 126 biological peptides, ACE2 was shown to hydrolyze with high catalytic efficiency the C-terminal residue of angiotensin II, apelin-13, and dynorphin A 1–13 (k_{cat}/K_m of about 2×10^6 M^{-1} s^{-1} for these peptides).[7] Based on its high catalytic efficiency in cleaving angiotensin II, it has been suggested that ACE2 counterbalances ACE function by regulating the level of angiotensin II produced by ACE.[8–11]

Physiological roles of ACE2 have been assessed by studying the effects of targeted disruption of the ACE2 gene in mice. In a first report, ACE2-deficient mice were reported to develop abnormal heart function.[12] In contrast, in a more recent study, no evidence was found for a role of ACE2 in the regulation of cardiac structure or function.[13] In this study, ACE2 was suggested to be a functional component of the RAS, contributing to the blood pressure regulation by modulation of angiotensin II levels in the kidneys. Differences in genetic backgrounds and the effects of general anesthesia on cardiac function have been proposed as possible causes for the observation of variable phenotypes between these two studies. The above results suggest that the complex interplay between ACE and ACE2 might be difficult to decipher using only genetic approaches. In addition to ACE2's role counterbalancing ACE function, through cleavage of the angiotensin II vasoconstrictor, the fact that vasodilators such as apelin might also be cleaved in vivo by ACE2 adds to the growing complexity of blood pressure regulation via RAS and other peptide signaling pathways.[14–16] The hypotensive response of apelin injection in rats was only transient, reflecting a rapid degradation of this peptide in the bloodstream, probably by ACE2.[17] In this regard, the deletion of the C-terminal phenylalanine residue of apelin 1–17 abolishes the hypotensive effect of this peptide, pointing out the crucial role played in vivo by a carboxypeptidase able to cleave this phenylalanine C-terminal residue.[17]

To clarify the functional roles of ACE2, it will be mandatory to identify its in vivo substrates. This objective can be approached by administration of selective ACE2 inhibitors to animals and screening for those peptides or the peptidome that are modified by specific ACE2 blockade. Millenium Pharmaceuticals has developed the first potent nonpeptide inhibitor of ACE2 (MLN-4760, $IC_{50} = 0.44$ nM, compound **I** in Scheme 1), which exhibits high selectivity (>5000) toward carboxypeptidase A (CPA).[18] The presence of two carboxylate groups in

Scheme 1. Chemical Structure of Compound **I**

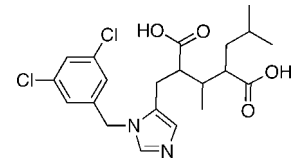

* To whom correspondence should be addressed. Tel.: 330169082603. Fax: 330169089071. E-mail: vincent.dive@cea.fr.

[†] University of Athens.

[‡] CEA, DSV.

[a] Abbreviations: ACE, angiotensin-converting enzyme; ACE2, angiotensin-converting enzyme 2; Ac_2O, acetic anhydride; AcOH, acetic acid; AcOEt, ethyl acetate; Boc, *tert*-butoxycarbonyl; *t*-Bu, *tert*-butyl; Cbz, benzyloxycarbonyl; CPA, carboxypeptidase A; DCM, dichloromethane; DMF, dimethylformamide; DMSO, dimethyl sulfoxide; DPM·H_3PO_2, aminodiphenylmethane hypophosphite; DpaOH, N^3-(2,4-dinitrophenyl)-L-diaminopropionyl; Dnp, 2,4-dinitrophenyl; Et_2O, diethyl ether; EtOH, ethanol; HMDS, 1,1,1,3,3,3-hexamethyldisilazane; MCA, (7-methoxycoumarin-4-yl)acetyl; MeOH, methanol; MMPs, matrix metalloproteinases; NCS, *N*-chlorosuccinimide; Np, *para*-nitrophenyl; P.E. 40–60 °C, petroleum ether 40–60 °C; TMSCl, chlorotrimethylsilane; TFA, trifluoroacetic acid.

10.1021/jm701275z CCC: $40.75
Published on Web 03/07/2008

Table 1. Potency of Phosphinic Peptide Inhibitors toward ACE2, CPA, and ACE

No.	compounds	ACE2 K_i nM	CPA K_i nM	ACE K_i
12	Cbz-**Pro**Ψ (PO_2-CH_2)**Phe**-OH	300		
13	Cbz-ProΨ (PO_2-CH_2)**Leu**-OH	300		
14	Cbz-ProΨ (PO_2-CH_2)**Ala**-OH	3000		
15	Cbz-**Ala**Ψ(PO_2-CH_2)Phe-OH	>10000		
16	Cbz-**Phe**Ψ (PO_2-CH_2)Phe-OH	>10000		
17	Cbz-**Leu**Ψ (PO_2-CH_2)Phe-OH	8000		
18	**Ala**Ψ (PO_2-CH_2)Phe-OH	>10000		
19	**Phe**Ψ (PO_2-CH_2)Phe-OH	>10000		
20	**Leu**Ψ (PO_2-CH_2)Phe-OH	>10 000		
26	**Pro**Ψ (PO_2-CH_2)Phe-OH	>10000		
27	Ac-**Ala**-ProΨ (PO_2-CH_2)Phe-OH	7.5		
28	Ac-**Leu**-ProΨ (PO_2-CH_2)Phe-OH	0.35		
28_{FII}	Ac-**Leu**-ProΨ (PO_2-CH_2)Phe-OH, FII	0.13	0.5	>10 μM
29	Ac-**Lys**-ProΨ (PO_2-CH_2)Phe-OH	6.5		
30	Ac-**Glu**-ProΨ (PO_2-CH_2)Phe-OH	7		
31	Ac-**Tyr**-ProΨ (PO_2-CH_2)Phe-OH	5.2		
32	Ac-**Phe**-ProΨ (PO_2-CH_2)Phe-OH	5.2		
33	Ac-**Val**-ProΨ (PO_2-CH_2)Phe-OH	6.6		
34	Ac-**His**-ProΨ (PO_2-CH_2)Phe-OH, FII	2.1		
34_{FII}	Ac-**His**-ProΨ (PO_2-CH_2)Phe-OH, FII	0.7	60	>10 μM
35	Ac-Leu-**Phe**Ψ (PO_2-CH_2)Phe-OH	920	0.3	
36	Ac-His-**Leu**Ψ (PO_2-CH_2)Phe-OH	800	175	
40_{FII}	Ac-Leu-ProΨ (PO_2-CH_2)**Isoxa(Phe)**[a]-OH	1.25	35	>10 μM
41_{FII}	Ac-His-ProΨ (PO_2-CH_2)**Isoxa(Phe)**[a] -OH	0.4	1050	>10 μM
44_{FII}	Ac-His-**Leu**Ψ (PO_2-CH_2)**Isoxa(Phe)**[a] -OH	220	>10 μM	

[a] Isoxa(Phe): 2-(3-phenyl-isoxazol-5-ylmethyl)-propionic acid.

I, which can interact with the zinc atom of the ACE2 active site, may lead to two binding modes of this inhibitor to ACE2 and may favor its interaction with other zinc metalloproteinases. In fact, in the crystal structure of **I** interacting with ACE2,[19] the experimental binding mode was opposite to that predicted,[18] with the substituted imidazole side chain pointing into the S_1' pocket and the Leu one into the S_1 subsite.

In vivo, full blockade of ACE2 required high doses of **I** (40 to 80 mg/kg/day in mice), suggesting low bioavailability of this compound.[20] This is in contrast to the phosphinic peptide ACE inhibitor dose of 10 mg/kg in mice, respectively, N- and C-domain selective ACE inhibitors, generally used to observe full blockade of angiotensin I conversion in vivo.[21] These observations on **I** led us to consider the development of potent and selective ACE2 inhibitors, based on phosphinic peptide chemistry. Previous studies have shown that phosphinic peptides, besides providing highly potent and selective zinc proteinase inhibitors, exhibit good bioavailability and are recovered intact, either in urine or feces.[21–23] Furthermore, crystal structures of these transition-state analogs interacting with their targeted zinc proteinases provide important clues about the active site residues that are critical for enzyme catalysis.[24–27]

Herein, we report the development of new class of potent ACE2 inhibitors, which are pseudopeptides containing a phosphinic moiety that mimics the structure of ACE2 peptide substrates in their transition states. After a first optimization step leading to potent ACE2 inhibitors, selectivity of the developed compounds was assessed by testing their potency toward CPA and ACE. The second step of optimization relied on the development of a model of interaction between one phosphinic peptide of this series and ACE2. This model enabled development of a compound exhibiting high selectivity toward CPA, while maintaining nanomolar potency toward ACE2. Other classes of ACE2 inhibitors have been reported, but the compounds identified either display low potency toward ACE2 (IC_{50} in the μM range)[28,29] or are not suitable for in vivo experiments (peptides identified by phage-display).[30]

Scheme 2. Possible Disconnections for Synthesis of Pseudoproline Containing Phosphinic Peptides

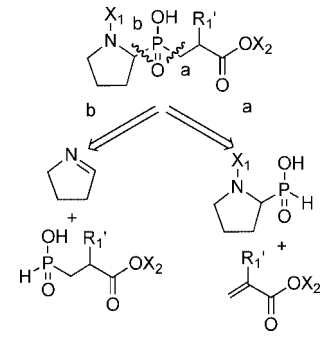

Results

Chemistry. Simple phosphinic pseudodipeptides were first synthesized to identify potent ACE2 inhibitors, among which compound **12** incorporates pseudoproline residue in the P_1 position (Table 1), as observed in the preferred peptide substrates of ACE2, angiotensin II, and apelin, where hydrolysis occurs between proline and phenyalanine. Phosphinic peptides containing a pseudoproline analogue in P_1 position were obtained using two methods, according to disconnections a and b (Scheme 2). By using method a, phosphinic blocks **3**–**5** were synthesized, from which compounds **12**–**14** (Scheme 3) were prepared, after removal of the X_2 protecting groups, in relatively low yields. Substantial improvement in yield was achieved by using method b (scheme 2), allowing the preparation of compound **3** in high yield (Scheme 4), which is also the basic precursor of phosphinic tripeptide inhibitors **27**–**34** (Scheme 5). Method b has also been used for the synthesis of the block that bears the propargyl side chain at P_1' position (compound **38**, Scheme 7), the precursor for the introduction of substituted isoxazole rings at this position (compound **39**, Scheme 7). Phosphinic inhibitors **15**–**17**, bearing the side chains of pseudo-Ala, -Phe, and - Leu, respectively,

Scheme 3. Synthesis of Phosphinodipeptide Inhibitors **12–20**[a]

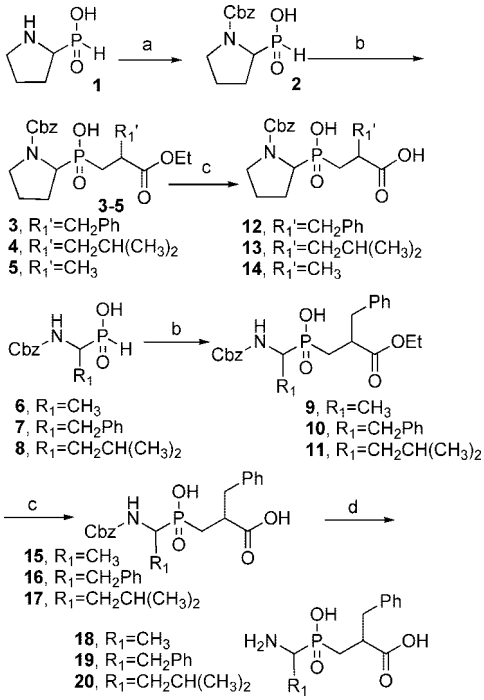

[a] Reagents, conditions, and yields: (a) aq Na_2CO_3, CbzCl (1.8 equiv), 0 °C to room temperature, 12 h, 80%; (b) HMDS (5 equiv), 110 °C, 1 h, under argon, $CH_2{=}C(R_1')COOEt$, (1.2 equiv), 4 h, then EtOH, **3** 52%, **4** 47%, **5** 49%, **9** 72%, **10** 81%, **11** 74%; (c) 1 M NaOH in MeOH, rt, 12 h, **12** 95%, **13** 96%, **14** 92%, **15** 88%, **16** 90%, **17** 95%; (d) H_2, 10% Pd/C in $MeOH/H_2O$ = 4/1, rt, 2 h, **18** 92%, **19** 95%, **20** 94%.

were synthesized using method a, which relies on well-established procedures developed previously.[31]

The assembly of tripeptide phosphinic inhibitors **27**−**36**, **40**, **41**, and **44** was achieved by coupling of L-amino acids with the suitable phosphinic dipeptide block, using the method of activated (nitrophenyl) esters, N_α-deprotection and acetylation, in such conditions that acetylation of the P-OH group did not happen. Because activation of fully deprotected phosphinic dipeptide blocks of type **18–20** would lead to autocondensation products, the nitrophenylester activation of the L-amino acids was the method of choice.

In detail, the proline-phosphinic acid analogue **1** was synthesized according to known procedures[32] and protected to give **2**. Michael-type addition of **2** to acrylates[33] led to compounds **3–5** in moderate to good yields. Accordingly, alanine, phenylalanine, and leucine-phosphinic acid analogues **6**, **7**, and **8** were added to the phenylalanine-like acrylate, leading to compounds **9**, **10**, and **11**, respectively. Saponification of compounds **3–5** and **9–11** afforded phosphinic peptides **12–17** in excellent yields. Catalytic hydrogenation of compounds **15–17** provided the unprotected analogues **18–20** in excellent yields, as shown in Scheme 3.

The key synthon **3** was alternatively synthesized by applying a "reverse" methodology (method b). Phosphinic acid **22** was used to attack 1-pyrroline trimer **21′**, thus leading to **3** after protection of the amino group.[34] This two-step approach proved to be much more convenient and high-yielding (52% overall) than method a, which applied the four-step synthesis of proline-phosphinic acid analogue **2** and its subsequent attack on acrylates with an overall yield of 6%.

Removal of the Cbz-group from compound **12** under catalytic hydrogenation conditions afforded **26** in 95% yield (Scheme 5). Coupling of **26** with the suitably protected natural amino acids Ala, Val, Lys, Glu, Tyr, Phe, Leu, and His was performed by using their corresponding reactive nitrophenyl esters. Removal of the N_α-protecting group, subsequent acetylation, and finally, deprotection of side chains provided inhibitors **27–34**.

Scheme 4. Improved Synthetic Procedure for **3**[a]

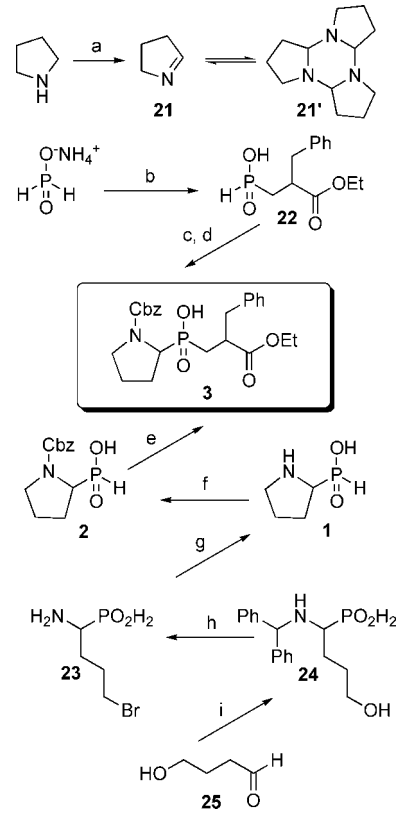

[a] Reagents, conditions, and yields: Method B, (a) 25% $Na_2S_2O_4$ (1 equiv), NaOH (2 equiv), $AgNO_3$ (0.05 equiv) in H_2O, 0 °C to rt, 3 h, 60%; (b) HMDS (1 equiv), 110 °C, 1 h, under argon, $CH_2{=}C(CH_2Ph)COOEt$, (0.2 equiv) in DCM, 0 °C to rt, 12 h, then EtOH, 89%; (c) TMSCl (4 equiv), Et_3N (4 equiv) in DCM, 0 °C to rt, 3 h, under argon, **21** (1.1 equiv) in DCM, 0 °C to rt, 12 h, then EtOH; (d) MgO (3 equiv), CbzCl (1.5 equiv) in H_2O/Et_2O, 0 °C to rt, 12 h, 52% for two steps; Method A, (e) HMDS (5 equiv), 110 °C, 1 h, under argon, $CH_2{=}C(CH_2Ph)COOEt$, (1.2 equiv), 4 h, then EtOH, 52%; (f) aq Na_2CO_3, CbzCl (1.8 equiv), 0 °C to rt, 12 h, 80%; (g) *N*,*N*-dimethyldodecylamine (2 equiv), tetrabutylammonium hydroxide 40% (2 drops) in DCM/H_2O = 1/1, rt, 12 h, 71%; (h) aq HBr 47%, reflux, 3 h, 74%; (i) $DPM{\cdot}H_3PO_2$ (1 equiv) in 1,4 dioxane, reflux, 5 h, 48%.

Scheme 5. Synthesis of Phosphinotripeptide Inhibitors **27–34**[a]

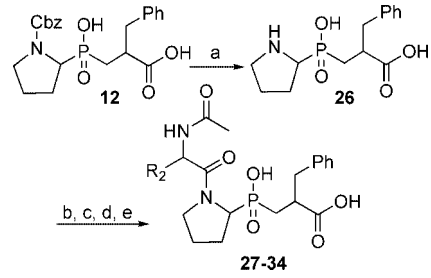

[a] Reagents, conditions, and yields: (a) H_2, 10% Pd/C in $MeOH/H_2O$ = 4/1, rt, 2 h, 95%; (b) $P_1NHCH(R_2)COONp$ (1.5 equiv), Et_3N (2 equiv) in DMF, rt, 12 h, 70–80%; (c) TFA/DCM, 50%, rt, 1 h, 90–95% or H_2, 10% Pd/C in $MeOH/H_2O$ = 4/1, rt, 2 h, 90–95% or HCOOH/DCM, 5%, rt, 10 min, 95%; (d) Ac_2O (3 equiv) in pyridine, rt, 12 h, 70–75%; (e) TFA/DCM, 50%, rt, 1 h, 90–95% when R_2 side chains correspond to those of alanine (**27**), leucine (**28**), lysine (**29**), glutamic acid (**30**), tyrosine (**31**), phenylalanine (**32**), valine (**33**), and histidine (**34**).

Scheme 6. Synthesis of Inhibitors **35** and **36**[a]

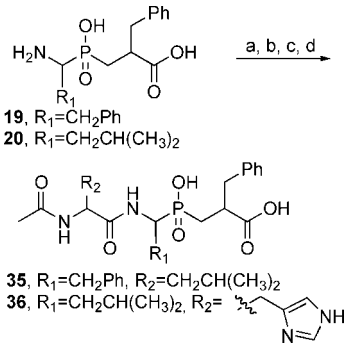

[a] Reagents, conditions, and yields: (a) BocLeuONp (1.5 equiv), Et_3N (2 equiv) in DMF, rt, 12 h, 75% for **19** and TrtHis(Trt)Onp 72% for **20**; (b) TFA/DCM, 50%, rt, 1 h, 90–95% for **19** and HCOOH/DCM 5% 10 min 90% for **20**; (c) Ac_2O (3 equiv) in pyridine, rt, 12 h, 70–75%; (d) TFA/DCM, 50%, rt, 1 h, 90% for **20**.

Scheme 7. Synthesis of Inhibitors **40** and **41**[a]

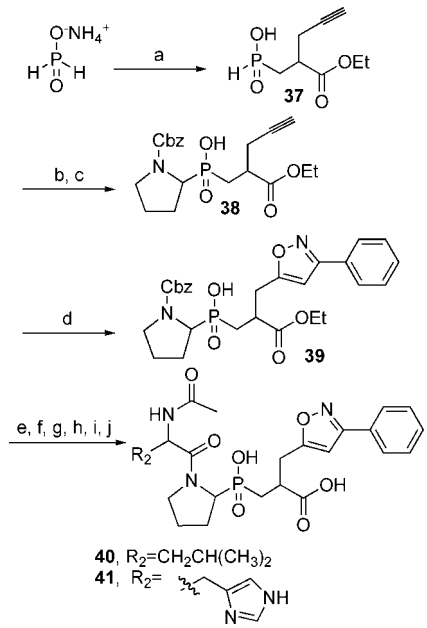

[a] Reagents, conditions and yields: (a) HMDS (1 equiv), 110 °C, 1 h, under argon, CH_2=C(CH_2C≡CH)COOEt, (0.2 equiv) in DCM, 0 °C to rt, 12 h, then EtOH, 88%; (b) TMSCl (4 equiv), Et_3N (4 equiv) in DCM, 0 °C to rt, 3 h, under argon, **21** (1.1 equiv), 0 °C to rt, 12 h, then EtOH; (c) MgO (3 equiv), CbzCl (1.5 equiv) in H_2O/Et_2O, 0 °C to rt, 12 h, 54% for two steps; (d) XCH=NOH (3 equiv), NCS (3 equiv), pyridine (0.74 equiv) in $CHCl_3$, 45 °C, 3 h, then **38**, Et_3N (3 equiv), 45 °C, 3 days, repeat 3 times, 80%; (e) 1 M NaOH in MeOH, rt, 12 h, 90%; (f) H_2, 10% Pd/C in MeOH/H_2O=4/1, rt, 2 h, 90%; (g) TrtHis(Trt)Onp 72% or BocLeuONp 75% (1.5 equiv), Et_3N (2 equiv) in DMF, rt, 12 h; (h) TFA/DCM, 50%, rt, 1 h, 90% or HCOOH/DCM 5%, rt, min, 92%; (i) Ac_2O (3 equiv) in pyridine, rt, 12 h, 70–75%; (j) TFA/DCM, 50%, rt, 1 h 90% for **41**.

When a similar methodology was used, phosphinic inhibitors **35** and **36** were synthesized (Scheme 6). Coupling of **19** and **20** with the suitably protected derivative of Leu and His, respectively, removal of the N_α-protecting group, subsequent acetylation, and finally, deprotection of side chains provided inhibitors **35** and **36**.

Isoxazole-containing phosphinic peptides were synthesized by applying two different methodologies (Schemes 7 and 8). Compound **38** (Scheme 7) was synthesized according to the improved strategy described in Scheme 4, whereas **42** (Scheme 8) was synthesized by standard methods. In both cases, 1,3-dipolar cycloadditions were achieved by similar procedures,

Scheme 8. Synthesis of Compound **44**[a]

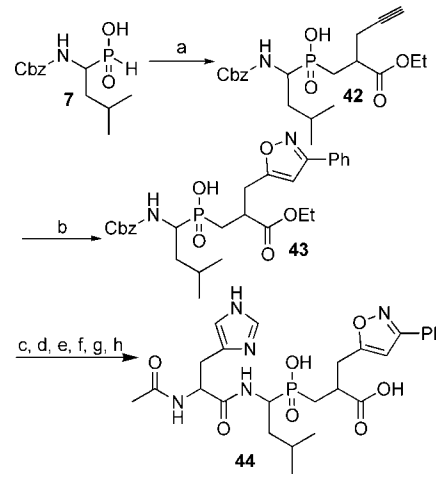

[a] Reagents, conditions, and yields: (a) HMDS (5 equiv), 110 °C, 1 h, under argon, CH_2=C(CH_2C≡CH)COOEt (1.2 equiv), 4 h, then EtOH, 98%; (b) PhCH=NOH (3 equiv), NCS (3 equiv), pyridine (0.74 equiv) in $CHCl_3$, 45 °C, 3 h, then **42**, Et_3N (3 equiv), 45 °C, 3 days, repeat 3 times, 83%; (c) 1 M NaOH in MeOH, rt, 12 h, 92%; (d) H_2, 10% Pd/C in MeOH/H_2O = 4/1, rt, 2 h, 95%; (e) TrtHis(Trt)ONp (1.5 equiv), Et_3N (2 equiv) in DMF, rt, 12 h, 78%; (f) HCOOH/DCM, 5%, rt, 1 h, 93%; (g) Ac_2O (3 equiv) in pyridine, rt, 12 h, 75%; (h) TFA/DCM, 50%, rt, 2 h, 90%.

leading to **39** and **43** in very good yields. Deprotection of the carboxylate and α-amino protecting groups, coupling with the natural amino acids (Leu for **40** and His for **41** and **44**), removal of the N_α-protecting group, subsequent acetylation, and finally, deprotection of side chains provided inhibitors **40** and **41** (Scheme 7) and **44** (Scheme 8).

ACE2 Inhibition. Phosphinic Dipeptides. Compound **12**, which mimics the Pro-Phe cleavage site observed in angiotensin II and apelin, behaved as a weak ACE2 inhibitor (Table 1, at this stage phosphinic peptides were tested as a mixture of four diastereoisomers). The potency displayed by compound **13** demonstrates that phenylalanine and leucine side chains are equally accepted by the ACE2 S_1' subsite. However, the presence of a small side chain like a methyl in the S_1' subsite (compound **14**) reduced the inhibitor affinity 10-fold. Substitution of the P_1 pseudoproline by pseudoalanine (**15**), pseudophenylalanine (**16**), or pseudoleucine (**17**) resulted in a marked affinity decrease, a result in agreement with the ACE2 preference to cleave substrate with a proline in the P_1 position. The low potency displayed by compounds **18**, **19**, **20**, and **26** reveals a key role of the Z group in potency, either through the phenyl ring or the oxycarbonyl group of this protecting function.

Phosphinic Tripeptides. The presence of a residue in the P_2 position of phosphinic compounds has a dramatic impact on potency, as compounds **27** to **34** all exhibited nanomolar potency. Elongation of **12** with Ac-Ala (**27**) increased the affinity by almost 2 orders of magnitude. ACE2 was observed to accommodate several residues in the P_2 position (**27**–**34**), as only a slight preference was observed for Leu and His residues at this position (**28** and **34**). Compounds **28** and **34** were resolved into four single diastereoisomers by HPLC purification. Testing the activity of these HPLC fractions revealed that only a single fraction exhibited inhibitory potency toward ACE2. The FII subscript reported in Table 1 indicates that the active diastereoisomer is the second fraction of the HPLC chromatogram. Substitution of the pseudoproline in P_1 position by Phe in this tripeptide series resulted in marked affinity reduction (**28** vs **35**). A similar decrease in affinity was observed when the pseudoproline in P_1 position of **34** was replaced by a leucine

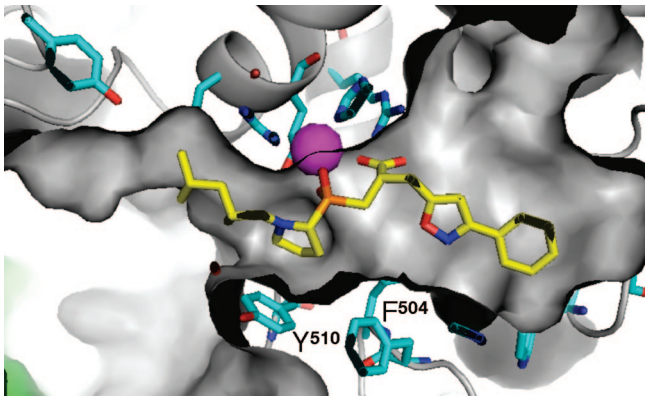

Figure 1. Surface representation of the ACE2 active site illustrating how the isoxazole-phenyl and the proline residues of compound **40** (yellow stick) fit into, respectively, the S_1' and S_1 subsites of ACE2. Tyr^{510} and Phe^{504} shaping the S_1 pocket appear in blue sticks under the inhibitor proline. The zinc atom is represented as a pink sphere.

(**36**). These results confirm the preference of ACE2 for a proline at this position, either in substrates or transition-state inhibitors. However, compounds **28** and **34** also turned out to be potent inhibitors of CPA (as other tripeptides in this series, data not shown). Interestingly, compound **34** with a histidine in P_2 position was less potent toward CPA, a result suggesting that this particular residue in the P_2 position can be used to control inhibitor selectivity toward ACE2.

Exploitation of the ACE2 S_1' Pocket. Analysis of the ACE2 three-dimensional structure in complex with compound **I** (Scheme 1) indicates that the S_1' pocket is a very large cavity, formed by the lengthwise channel between the two ACE2 subdomains. This observation partly explains the unanticipated binding mode of compound **I** that places the bulky dichlorobenzyl imidazole side chain in the S_1' cavity and the isobutyl group in the narrower S_1 pocket of ACE2.[5] The particular size of the ACE2 S_1' cavity led us to develop phosphinic peptides comprising longer side chains in their P_1' position as a way to restrict their potency toward ACE2. The potential interest in such compounds was further supported by the fact that, in contrast to ACE2, CPA contains a much smaller S_1' cavity. Modeling studies with different phosphinic compounds harboring long side chains in their P_1' position led us to select compounds containing an isoxazole ring substituted by a phenyl in the P_1' position, like in compound **40** (Scheme 7). As illustrated in Figure 1, such a side chain fills part of the S_1' cavity of ACE2, with no apparent steric clash. In agreement with this model, compound **40**, as compared with compound **28**, behaved as a potent ACE2 inhibitor. In contrast, for CPA, the replacement of a phenyl by a phenyl-isoxazole side chain reduced inhibitory potency 70-fold (compound **28** vs **40**). The same trends were observed for compound **41**, a potent inhibitor of ACE2 ($K_i = 0.4$ nM) able to discriminate ACE2 from CPA with a selectivity factor higher than 3 orders of magnitude. Replacing the pseudoproline of **41** with a leucine in **44** resulted in marked affinity decrease, a result pointing out again the critical importance of this residue for good ACE2 inhibitory potency.

Finally it is worth noting that compounds **28**, **34**, and **41** display no potency toward ACE when tested at concentration of 10 μM, an expected result, as the presence of a P_2' residue is a strict requirement for potent inhibition of this dipeptidyl carboxypeptidase enzyme.

Discussion

In this study, we demonstrate that phosphinic peptides with optimal side-chain content behave as highly potent inhibitors of ACE2. High potency was observed to depend on some key structural features of these phosphinic peptides. In the following, the role of these structural features is tentatively discussed in the light of the X-ray structure of ACE2 in interaction with compound **I**, and the predicted model of interaction of compound **40** with ACE2. The X-ray structure of the ACE2 complex reveals that the S_1 subsite of this enzyme is a small pocket, defined by the side-chain of four residues The^{347}, Phe^{504}, Tyr^{510}, and Arg^{514}.[5] Based on this structure, both leucine and proline side chains were proposed to ideally fit with the S_1 subsite of ACE2. While the high potency displayed by compounds containing a pseudoproline in the inhibitor P_1 position (**34** and **41**) fits well with this proposal, the dramatic loss of potency observed when the P_1 proline is replaced by a leucine (compounds **34** vs **36** and **40** vs **44**) is more unexpected. The conformational restriction imposed by the presence of a pseudoproline in these inhibitors may account for their greater potency than inhibitors containing a leucine in the P_1 position. However, less optimal van der Waals contacts associated with the binding of inhibitors containing a leucine in the P_1 position cannot be completely excluded. In fact, in our model between the ACE2 and compound **40**, the proline side chain is in close contact with Phe^{504} and Tyr^{510}, in a binding mode that should provide tight van der Waals interactions. Based on this model, proline substitution by leucine in a phosphinic peptide would imply a steric clash between the δCH_3 of leucine side chain and the phenolic side chain of Tyr^{510} and, thus, an energetic cost to move Tyr^{510}. It should be kept in mind that compound **I** is not a transition-state analog, so, in contrast with phosphinic peptides, the topology of the leucine side chain, as observed in the X-ray structure of this inhibitor, is not expected to reflect exactly the topology assumed by the P_1 side chain of a substrate in the transition state. Overall, the nice fit observed in our ACE2 model between the proline residue and the S_1 pocket of ACE2 may explain the critical role of this residue in the potency of phosphinic inhibitor, as well as substrate specificity reported for ACE2. Interestingly, the Tyr^{510} in ACE2 is replaced by a smaller side chain in ACE (Val^{518}), a mutation probably explaining the unique P_1 specificity of ACE2.

Acylation of proline by a benzyloxycarbonyl group significantly improves inhibitor potency (compound **12** vs **26**). Based on our model, it can be predicted that in the bound state the carbonyl oxygen of this group should be within H-bond distance of the NH backbone of Ala^{348}. Interestingly, the same interaction is also observed in the X-ray structure of ACE in complex with the RXPA380 inhibitor, between the Z-group of the inhibitor P_1 residue (Z-Phe) and NH of Ala^{356} in ACE.[26] The topology of this alanine residue is strictly conserved between ACE and ACE2. Finally, high potency in this series requires the presence of a residue in the P_2 position of the inhibitors. In our model, the inhibitor P_2 side chain points toward a large cavity defined by His^{378}, His^{401}, and Asp^{382} residues. No specific interactions between the inhibitor P_2 side chain and ACE2 residues could be predicted according to our model. This observation fits with our results showing that various inhibitor P_2 side chains are well tolerated by ACE2. In contrast, two specific interactions involving P_2 backbone atoms are observed in the model. Indeed, the NH of Leu and the carbonyl of the acetyl group are

H-bonded to, respectively, the carbonyl of Ala^{348} and the hydroxyl of Tyr^{510}. These H-bonding interactions may account for the dramatic difference in potency observed between pseudodipeptides and pseudotripeptides in this series of inhibitors.

Despite the presence of a pseudoproline in most inhibitor structures, CPA also was observed to bind such unusual proline-containing inhibitors with high potency. Selectivity for ACE2 was achieved, on the one hand, by exploiting the unusual size of the S_1' subsite of ACE2 and, on the other hand, by exploiting the nature of the P_2 residue. While ACE2 was observed to accommodate several residues in the P_2 position, the presence of a histidine in this position produces inhibitors (**34** and **41**) displaying reduced potency toward CPA. The high selectivity of compound **41** was obtained by combining both a histidine in the P_2 position and a long side chain in the P_1' position pointing into the unusual large S_1' cavity of ACE2.

Previous studies have demonstrated that phosphinic peptide inhibitors, due to remarkable in vivo stability, can be used to probe the in vivo function of zinc metalloproteinases.[21–23] Thus, compound **41** developed in this study should be a suitable tool to define the physiological substrates of ACE2. Numerous natural peptides have been proposed as physiological substrates of ACE2, like angiotensin II and apelin; however, up to now, the effect of ACE2 blockade by specific inhibitors on the levels of these peptides in animal models has never been studied quantitatively. Such studies are mandatory to improve our basic knowledge of ACE2 and to define pharmacological applications for ACE2 specific inhibitors, as those reported here.

Experimental Section

General Procedures. All of the compounds, for which analytical and spectroscopic data are quoted, were homogeneous by TLC. TLC analyses were performed using silica gel plates (E. Merck silica gel 60 F-254) and components were visualized by the following methods: ultraviolet light absorbance, charring after spraying with a solution of $(NH_4)HSO_4$, ninhydrin, and Pauli tests. The solvent systems used for TLC developments were (a) $CHCl_3$−MeOH−AcOH (7:2:1) and (b) $CHCl_3$−MeOH−AcOH (7:0.5:0.5). Column chromatography was carried out on silica gel (E. Merck, 70−230 mesh), height 35 cm, diameter 1.2 cm.

Phosphinic peptide purity was established by analytical HPLC and mass spectrometry. ESI mass spectral analysis was performed either on a mass spectrometer MSQ Surveyor, Finnigan at the Laboratory of Organic Chemistry, University of Athens, using direct sample injection, or on a Micromass Platform II instrument, Atheris Laboratories, Geneva, Switzerland. Negative or positive ion ESI spectra were acquired by adjusting the needle and cone voltages accordingly. HPLC analyses and preparative purifications were carried out on a MZ-analytical column 250 × 4 mm, Kromasil, 100, C18, 5 μm, at a flow rate of 0.5 mL/min. Solvent A: 10% CH_3CN, 90% H_2O, 0.1% TFA. Solvent B: 90% CH_3CN, 10% H_2O, 0.09% TFA.. Eluted peaks were detected at 254 nm. Given times correspond to one or two diastereoisomeric forms and are counted in minutes.

^1H, ^{13}C, and ^{31}P NMR spectra were recorded on a 200 MHz Mercury Varian spectrometer. All NMR experiments were carried at 298 K. ^{13}C and ^{31}P NMR spectra are fully proton decoupled. ^{31}P chemical shifts are reported on δ scale, in ppm, downfield from 85% H_3PO_4.

Detailed experimental procedures leading to compounds **1**, **6**–**8**, **23**–**25**,[17] and **22**[20] have been described elsewhere.

Chemistry. 2-Hydroxyphosphinoyl-pyrrolidine-1-carboxylic Acid Benzyl Ester (2). CbzCl (5.7 mmol, 0.97 g, 0.82 mL) was added dropwise at 0 °C to a solution of **1** (5.2 mmol, 0.7 g) in 10% aq Na_2CO_3 (10 mL). The reaction mixture was stirred for 10 h at rt and another 0.6 equiv of CbzCl was added and stirred at rt for 2 h. NaOH (4 M) was added to bring the pH to 12 and the reaction mixture was washed with Et_2O (2 × 10 mL). Acidification with 2 M HCl to pH = 1, extraction with AcOEt (2 × 30 mL), and removal of solvent afforded the product as colorless oil. Yield: 80%. TLC R_f (a) 0.37. HPLC (Gradient: t = 0 min 0% B, t = 10 min 25% B, t = 45 min 75% B, t = 50 min 100% B) t_R = 18.22 min. ^1H NMR (200 MHz, $CDCl_3$) δ 1.73–2.24 (m, 4H), 3.23–3.54 (m, 2H), 3.88–3.98 (m, 1H), 5.04–5.13 (m, 2H), 6.96 (d, $^1J_{PC}$ = 540 Hz, 1H), 7.10 (d, $^1J_{PC}$ = 540 Hz, 1H), 7.28–7.44 (m, 5H); ^{13}C NMR (50 MHz, $CDCl_3$) δ 23.81, 24.15, 24.75, 29.46, 46.81, 47.13, 55.25 (d, $^1J_{PC}$ = 110.12 Hz), 55.98 (d, $^1J_{PC}$ = 110.12 Hz), 67.23, 127.68, 127.9, 128.3, 136.07, 155.37; ^{31}P NMR (81 MHz, $CDCl_3$) δ 30.05, 31.09; ESMS m/z calcd for $C_{12}H_{17}NO_4P$ $(M + H)^+$, 270.1; found, 270.1.

2-[(2-Ethoxycarbonyl-3-phenyl-propyl)-hydroxy-phosphinoyl]-pyrrolidine-1-carboxylic Acid Benzyl Ester (3). Method A (Scheme 1): A suspension of **2** (2.6 mmol, 0.7 g) and HMDS (13 mmol, 2 g, 2.56 mL) was heated at 110 °C for 1 h under an argon atmosphere. Acrylate CH_2═C(CH_2Ph)COOEt (3.12 mmol, 0.58 g) was added at this temperature dropwise for 15 min, and the reaction mixture was stirred for 4 h. Then, absolute EtOH (5 mL) was added dropwise at 70 °C. After cooling at room temperature, the mixture was evaporated in vacuo. The residue was dissolved in AcOEt (30 mL), and the resulting suspension was washed with 1 M HCl (2 × 10 mL). Purification by column chromatography, using $CHCl_3$−MeOH−AcOH (7:0.3:0.3) as eluent, afforded the product as white foam. Yield: 52%. Method B (Scheme 2): Et_3N (108 mmol, 10.9 g, 15.25 mL) and TMSCl (108 mmol, 11.7 g, 13.7 mL) were added to a solution of **16** (27 mmol, 7 g) in dry DCM (180 mL) at 0 °C under an argon atmosphere. After 3 h at rt, the reaction mixture was cooled to 0 °C and **15** (30 mmol, 6.2 g) in dry DCM (20 mL) was added dropwise. The reaction mixture was stirred at rt for 12 h and then abs. EtOH (15 mL) was added dropwise. Removal of solvent afforded crude **20**, which was dissolved in H_2O/Et_2O (80/5 mL), and MgO (81 mmol, 3.26 g) was added. After cooling to 0 °C, CbzCl (40.5 mmol, 6.91 g, 5.8 mL) was added dropwise and the reaction mixture was stirred for 12 h at rt. Acidification with 2 M HCl to pH = 1, extraction with AcOEt (3 × 200 mL), drying over Na_2SO_4, and removal of solvent afforded the crude product. Purification by column chromatography, using $CHCl_3$−MeOH−AcOH (7:0.3:0.3) as eluent, afforded the product as white foam. Yield: 52%. TLC R_f(b) 0.52. HPLC (gradient t = 0, 0% B; t = 10, 35% B; t = 35, 100% B) t_R = 26.26, 26.63 min. ^1H NMR (200 MHz, $CDCl_3$) δ 0.97–1.14 (m, 3H), 1.67–2.44 (m, 6H), 2.68–3.23 (m 3H), 3.35–3.68 (m, 2H), 3.87–4.24 (m, 3H), 5.02–5.20 (m, 2H), 6.99–7.47 (m, 10H); ^{13}C NMR (50 MHz, $CDCl_3$) δ 13.84, 23.54, 24.50, 25.16, 25.91, 29.62 (d, $^1J_{PC}$ = 91.86 Hz), 39.50, 40.87, 47.06, 55.84 (d, $^1J_{PC}$ = 107.7 Hz), 56.59 (d, $^1J_{PC}$ = 107.7 Hz), 60.37, 67.34, 126.37, 127.77, 128.01, 128.2, 128.40, 129.0, 136.10, 138.03, 155.70, 173,4; ^{31}P NMR (81 MHz, $CDCl_3$) δ 56.15, 56.01; ESMS m/z calcd for $C_{24}H_{31}NO_6P$ $(M - H)^-$, 458.2; found, 458.5.

2-[(2-Ethoxycarbonyl-4-methyl-pentyl)-hydroxy-phosphinoyl]-pyrrolidine-1-carboxylic Acid Benzyl Ester (4). Same experimental procedure as for **3**, method A, using CH_2═C(CH_2CH-(CH_3)$_2$)COOEt, afforded product as white foam. Yield 47%. TLC R_f (b) 0.48. HPLC (t = 0 min, 0% B; t = 10 min, 25% B; t = 45 min, 75% B; t = 50 min, 100% B) t_R = 38.08, 38.80 min. ^1H NMR (200 MHz, $CDCl_3$) δ 0.74–1.02 (m, 6H), 1.07–1.72 (m, 6H), 1.78–2.47 (m 6H), 2.71–3.02 (m, 1H), 3.37–3.71 (m, 2H), 4.01–4.22 (m, 3H), 5.05–5.23 (m, 2H), 7.22–7.48 (m, 10H); ^{13}C NMR (50 MHz, $CDCl_3$) δ 13.92, 21.69, 22.64, 23.47, 24.50, 25.17, 25.65, 30.35 (d, $^1J_{PC}$ = 88.9 Hz), 30.60 (d, $^1J_{PC}$ = 88.9 Hz), 36.94, 43.46, 46.99, 55.92 (d, $^1J_{PC}$ = 106.34 Hz), 56.64 (d, $^1J_{PC}$ = 106.34 Hz), 60.33, 67.24. 127.73, 127.99, 128.33, 136.33, 155.54, 174.86; ^{31}P NMR (81 MHz, $CDCl_3$) δ 56.53, 56.06; ESMS m/z calcd for $C_{21}H_{33}NO_6P$ $(M - H)^-$, 424.2; found, 426.4.

2-[(2-Ethoxycarbonyl-propyl)-hydroxy-phosphinoyl]-pyrrolidine-1-carboxylic Acid Benzyl Ester (5). Same experimental procedure as for **3**, method a, using CH_2═C(CH_3)COOEt, afforded product as white foam. Yield 49%. TLC R_f (b) 0.36. HPLC (gradient t = 0, 0% B; t = 10, 35% B; t = 35, 100% B) t_R = 21.02, 20.90 min. ^1H NMR (200 MHz, $CDCl_3$) δ 1.13–1.37 (m, 6H), 1.77–2.51 (m, 6H), 2.73–3.01 (m 1H), 3.39–3.72 (m, 2H), 4.06–4.25 (m, 3H),

5.03–5.26 (m, 2H), 7.18–7.53 (m, 5H); ^{13}C NMR (50 MHz, $CDCl_3$) δ 13.96, 19.19, 23.56, 24.54, 25.26, 25.83, 31.00 (d, $^1J_{PC}$ = 89.98 Hz), 31.30 (d, $^1J_{PC}$ = 89.98 Hz), 33.61, 47.13, 56.13 ((d, $^1J_{PC}$ = 107.12 Hz), 56.61 (d, $^1J_{PC}$ = 107.12 Hz), 60.64, 67.38, 127.80, 128.05, 128.44, 136.35, 155.74, 175.31; ^{31}P NMR (81 MHz, $CDCl_3$) δ 56.13, 55.90; ESMS *m/z* calcd for $C_{18}H_{27}NO_6P$ $(M + H)^+$, 384.1; found, 384.1.

2-Benzyl-3-[(1-benzyloxycarbonylamino-ethyl)-hydroxy-phosphinoyl]-propionic Acid Ethyl Ester (9). Same experimental procedure as for **3**, method a, using **6**, afforded product as white solid. Yield 72%. TLC R_f (b) 0.64. HPLC (gradient t = 0, 0% B; t = 10, 35% B; t = 35, 100% B) t_R = 24.51, 24.67 min. ^{1}H NMR (200 MHz, $CDCl_3$) δ 0.98–1.12 (m, 3H), 1.18–1.42 (m, 3H), 1.68–1.97 (m 1H), 2.02–2.29 (m, 1H), 2.74–3.17 (m, 3H), 3.88–4.11 (m, 3H), 4.97–5.18 (m, 2H), 6.99–7.43 (m, 10H); ^{13}C NMR (50 MHz, $CDCl_3$) δ 13.93, 14.07, 27.73 (d, $^1J_{PC}$ = 91.9 Hz), 39.64, 40.83, 45.06 (d, $^1J_{PC}$ = 104.64 Hz), 45.80 (d, $^1J_{PC}$ = 104.64 Hz), 60.84, 67.20, 126.72, 128.05, 128.08, 128.18, 128.41, 128.50, 129.04, 136.18, 137.72, 155.84, 174.05; ^{31}P NMR (81 MHz, $CDCl_3$) δ 54.42, 54.68; ESMS *m/z* calcd for $C_{22}H_{29}NO_6P$ $(M + H)^+$, 434.2; found, 434.3.

2-Benzyl-3-[(1-benzyloxycarbonylamino-2-phenyl-ethyl)-hydroxy-phosphinoyl]-propionic Acid Ethyl Ester (10). Same experimental procedure as for **3**, method a, using **7**, afforded product as white solid. Yield 81%. TLC R_f (b) 0.58. HPLC (gradient t = 0, 0% B; t = 10, 25% B; t = 45, 75% B; t = 50, 100% B) t_R = 41.96, 42.31 min. ^{1}H NMR (200 MHz, $CDCl_3$) δ 0.95–1.19 (m, 3H), 1.69–1.98 (m, 1H), 2.03–2.29 (m, 1H), 2.68–2.96 (m, 3H), 3.01–3.35 (m, 2H), 3.88–4.15 (m, 2H), 4.15–4.39 (m, 1H), 4.78–5.09 (m, 2H), 6.94–7.43 (m, 15H); ^{13}C NMR (50 MHz, $CDCl_3$) δ 13.74, 28.21 (d, $^1J_{PC}$ = 96.66 Hz), 33.87, 39.59, 40.86, 50.77 (d, $^1J_{PC}$ = 109.39 Hz), 51.70 (d, $^1J_{PC}$=109.39 Hz), 60.84, 66.74, 126.53, 127.62, 127.87, 128.29, 128.95, 129.11, 136.27, 136.66, 137.65, 156.45, 174.10; ^{31}P NMR (81 MHz, $CDCl_3$) δ 53.79, 54.25; ESMS *m/z* calcd for $C_{28}H_{33}NO_6P$ $(M + H)^+$, 510.2; found, 510.1.

2-Benzyl-3-[(1-benzyloxycarbonylamino-3-methyl-butyl)-hydroxy-phosphinoyl]-propionic Acid Ethyl Ester (11). Same experimental procedure as for **3**, method a, using **8**, afforded product as white solid. Yield 81%. TLC R_f (b) 0.58. HPLC (gradient t = 0, 0% B; t = 10, 25% B; t = 45, 75% B; t = 50 100% B) t_R = 39.42, 39.83 min. ^{1}H NMR (200 MHz, d_6-DMSO) δ 0.68–1.11 (m, 9H), 1.32–2.15 (m, 5H), 2.64–3.15 (m, 3H), 3.62–4.08 (m, 3H), 4.94–5.19 (m, 2H), 7.04–7.46 (m, 10H); ^{13}C NMR (50 MHz, $CDCl_3$) δ 13.86, 21.00, 23.46, 24.39, 27.88 (d, $^1J_{PC}$ = 94.94 Hz), 36.18, 39.62, 40.76, 47.73 (d, $^1J_{PC}$ = 106.75 Hz), 48.60 (d, $^1J_{PC}$ = 106.75 Hz), 60.69, 67.13, 126.57, 127.89, 128.07, 128.35, 128.46, 129.09, 136.29, 137.80, 156.11, 174.07; ^{31}P NMR (81 MHz, d_6-DMSO) δ 46.37, 46.25; ESMS *m/z* calcd for $C_{25}H_{35}NO_6P$ $(M + H)^+$, 476.2; found, 476.3.

2-[(2-Carboxy-3-phenyl-propyl)-hydroxy-phosphinoyl]-pyrrolidine-1-carboxylic Acid Benzyl Ester (12). NaOH (4 M, 6 mL) was added to a solution of **3** (1.52 mmol, 0.7 g) in MeOH (16 mL), and the reaction mixture was stirred at rt for 12 h. Removal of MeOH, dilution with H_2O (10 mL), washings with Et_2O (2 × 10 mL), acidification with 2 M HCl to pH = 1, extraction with AcOEt (2 × 20 mL), and removal of solvent afforded the product as white solid. Yield: 74%. TLC R_f (b) 0.27. HPLC (gradient t = 0, 0% B; t = 10, 25% B; t = 45, 75% B; t = 50, 100% B) t_R = 29.50, 30.01 min. ^{1}H NMR (200 MHz, $CDCl_3$) δ 1.62–2.41 (m, 6H), 2.68–3.19 (m, 3H), 3.24–3.66 (m 2H), 3.95–4.20 (m, 1H), 4.92–5.19 (m, 2H), 6.91–7.55 (m, 10H); ^{13}C NMR (50 MHz, DMSO) δ 23.38, 24.28, 24.99, 25.74, 29.86 (d, $^1J_{PC}$ = 80.84 Hz), 46.79, 56.18 (d, $^1J_{PC}$ = 106.1 Hz), 66.44, 126.34, 127.71, 127.91, 128.25, 128.48, 129.05, 136.97, 138.90, 154.78, 175.29; ^{31}P NMR (81 MHz, DMSO-d_6) δ 46.23, 47.17; ESMS *m/z* calcd for $C_{22}H_{25}NO_6P$ $(M - H)^-$, 430.1; found, 430.0.

2-[(2-Carboxy-4-methyl-pentyl)-hydroxy-phosphinoyl]-pyrrolidine-1-carboxylic Acid Benzyl Ester (13). Same experimental procedure as for **12** using **4**, afforded product as white solid. Yield 96%. TLC R_f (b) 0.36. HPLC (gradient t = 0, 0% B; t = 10, 25% B; t = 45, 75% B; t = 50, 100% B) t_R = 28.31, 29.79 min. ^{1}H NMR (200 MHz, DMSO-d_6) δ 0.65–0.97 (m, 6H), 1.04–1.23 (m, 1H), 1.27–1.56 (m 3H), 1.67–2.25 (m, 6H), 2.56–2.80 (m, 1H), 3.12–3.37 (m, 1H), 3.42–3.62 (m, 1H), 3.88–4.09 (m, 1H), 4.97–5.18 (m, 2H), 7.23–7.46 (m, 5H); ^{13}C NMR (50 MHz, DMSO-d_6) δ 21.78, 23.03, 24.28, 24.96, 25.48, 30.97 (d, $^1J_{PC}$ = 86.39 Hz) 36.98, 42.81, 46.88, 56.19 (d, $^1J_{PC}$ = 107.34 Hz), 66.35, 127.61, 127.91, 128.50, 136.99, 154.77, 176.42; ^{31}P NMR (81 MHz, DMSO-d_6) δ 46.29, 47.11; ESMS *m/z* calcd for $C_{19}H_{27}NO_6P$ $(M - H)^-$, 396.2; found, 396.5.

2-[(2-Carboxy-propyl)-hydroxy-phosphinoyl]-pyrrolidine-1-carboxylic Acid Benzyl Ester (14). Same experimental procedure as for **12** using **5**, afforded product as white solid. Yield 92%. TLC R_f (b) 0.28. HPLC (gradient t = 0, 0% B; t = 10, 25% B; t = 45, 75% B; t = 50, 100% B) t_R = 20.11, 20.35 min. ^{1} H NMR (200 MHz, DMSO-d_6) δ 0.97–1.30 (m, 3H), 1.53–2.31 (m, 6H), 2.57–2.81 (m 1H), 3.15–3.61 (m, 2H), 3.91–4.12 (m, 1H), 4.93–5.20 (m, 2H), 7.18–7.49 (m, 5H); ^{13}C NMR (50 MHz, DMSO-d_6) δ 18.75, 23.31, 24.30, 24.96, 25.82, 31.56 (d, $^1J_{PC}$ = 89.65 Hz), 33.22, 46.69, 56.15 (d, $^1J_{PC}$ = 105.44 Hz), 56.55 (d, $^1J_{PC}$ = 105.44 Hz), 66.36, 127.58, 127.89, 128.45, 136.88, 154.76, 176.72; ^{31}P NMR (81 MHz, d$_6$-DMSO) δ 46.28, 47.17; ESMS *m/z* calcd for $C_{16}H_{21}NO_6P$ $(M - H)^-$, 354.1; found, 354.3.

2-Benzyl-3-[(1-benzyloxycarbonylamino-ethyl)-hydroxy-phosphinoyl]-propionic Acid (15). Same experimental procedure as for **12** using **9**, afforded product as white solid. Yield 88%. TLC R_f (b) 0.33. HPLC (gradient t = 0, 0% B; t = 10, 25% B; t = 45, 75% B; t = 50, 100% B) t_R = 26.73, 26.95 min. ^{1}H NMR (200 MHz, DMSO-d_6) δ 1.07–1.33 (m, 3H), 1.59–1.82 (m, 1H), 1.88–2.10 (m, 1H), 2.78–3.08 (m, 3H), 3.67–3.92 (m, 1H), 4.96–5.12 (m, 2H), 7.06–7.41 (m, 10H); ^{13}C NMR (50 MHz, DMSO-d_6) δ 13.98, 27.36 (d, $^1J_{PC}$ = 89.04 Hz), 27.74 (d, $^1J_{PC}$ = 89.04 Hz), 46.70 (d, $^1J_{PC}$ = 106.14 Hz), 46.18 (d, $^1J_{PC}$ = 106.14 Hz), 65.66, 126.38, 127.68, 127.77, 127.88, 128.26, 128.45, 129.08, 129.12, 137.15, 138.93, 155.96, 175.33; ^{31}P NMR (81 MHz, DMSO-d_6) δ 46.83; ESMS *m/z* calcd for $C_{20}H_{23}NO_6P$ $(M - H)^-$, 404.1; found, 404.3.

2-Benzyl-3-[(1-benzyloxycarbonylamino-2-phenyl-ethyl)-hydroxy-phosphinoyl]-propionic Acid (16). Same experimental procedure as for **12** using **10**, afforded product as white solid. Yield 90%. TLC R_f (b) 0.38. HPLC (gradient t = 0, 0% B; t = 10, 25% B; t = 45, 75% B; t = 50, 100% B) t_R = 34.45, 34.67 min. ^{1}H NMR (200 MHz, DMSO-d_6) δ 1.59–1.85 (m, 1H), 1.87–2.13 (m, 1H), 2.60–3.15 (m, 5H), 3.76–3.99 (m, 1H), 4.88–4.96 (m, 2H), 7.02–7.42 (m, 15H); ^{13}C NMR (50 MHz, DMSO-d_6) δ 28.06 (d, $^1J_{PC}$ = 88.47 Hz), 27.68 (d, $^1J_{PC}$ = 88.47 Hz), 32.78, 52.07 (d, $^1J_{PC}$ = 104.56 Hz), 52.63 (d, $^1J_{PC}$ = 104.56 Hz), 65.18, 126.27, 126.36, 127.02, 127.08, 127.60, 128.20, 128.27, 129.10, 137.31, 138.49, 138.88, 156.16, 175.34; ^{31}P NMR (81 MHz, DMSO-d_6) δ 45.96; ESMS *m/z* calcd for $C_{26}H_{27}NO_6P$ $(M - H)^-$, 480.2; found, 480.4.

2-Benzyl-3-[(1-benzyloxycarbonylamino-3-methyl-butyl)-hydroxy-phosphinoyl]-propionic Acid (17). Same experimental procedure as for **12** using **11**, afforded product as white solid. Yield 95%. TLC R_f (b) 0.38. HPLC (gradient t = 0, 0% B; t = 10, 25% B; t = 45, 75% B; t = 50, 100% B) t_R = 34.77 min. ^{1}H NMR (200 MHz, DMSO-d_6) δ 0.68–1.00 (m, 6H), 1.30–1.77 (m, 4H), 1.82–2.09 (m, 1H), 2.74–3.03 (m, 3H), 3.64–3.86 (m, 1H), 4.98–5.19 (m, 2H), 7.07–7.42 (m, 10H); ^{13}C NMR (50 MHz, DMSO-d_6) δ 20.88, 23.37, 24.08, 27.41 (d, $^1J_{PC}$ = 87.28 Hz), 27.8 (d, $^1J_{PC}$ = 88.6 Hz), 35.75, 48.53 (d, $^1J_{PC}$ = 107.12 Hz), 49.01 (d, $^1J_{PC}$ = 107.12 Hz), 65.57, 126.33, 127.49, 127.59, 127.82, 128.23, 128.39, 129.08, 137.27, 156.40, 175.31; ^{31}P NMR (81 MHz, DMSO-d_6) δ 46.96; ESMS *m/z* calcd for $C_{23}H_{31}NO_6P$ $(M + H)^+$, 448.2; found, 448.1

3-[(1-Amino-ethyl)-hydroxy-phosphinoyl]-2-benzyl-propionic Acid (18). Pd/C (10%, 120 mg) was added to a solution of **15** (1 mmol, 405 mg) in MeOH/H_2O (20/5 mL) and AcOH (2 drops) at 0 °C. The reaction mixture was stirred for 2 h under H_2, at rt and 1 atm, and then filtered through a pad of celite. Removal of

solvents afforded the product as white solid. Yield: 92%. TLC R_f (a) 0.27; ESMS *m/z* calcd for $C_{12}H_{19}NO_4P$ $(M + H)^+$, 272.2; found, 272.3.

3-[(1-Amino-2-phenyl-ethyl)-hydroxy-phosphinoyl]-2-benzyl-propionic Acid (19). Pd/C (10%, 120 mg) was added to a solution of **16** (1 mmol, 480 mg) in MeOH/H_2O (20/5 mL) and AcOH (2 drops) at 0 °C. The reaction mixture was stirred for 2 h under H_2, at rt and 1 atm, and then filtered through a pad of celite. Removal of solvents afforded the product as white solid. Yield: 95%. TLC R_f (a) 0.27; ESMS *m/z* calcd for $C_{18}H_{23}NO_4P$ $(M + H)^+$, 348.1; found, 348.1

3-[(1-Amino-3-methyl-butyl)-hydroxy-phosphinoyl]-2-benzyl-propionic Acid (20). Pd/C (10%, 120 mg) was added to a solution of **17** (1 mmol, 450 mg) in MeOH/H_2O (20/5 mL) and AcOH (2 drops) at 0 °C. The reaction mixture was stirred for 2 h under H_2, at rt and 1 atm, and then filtered through a pad of celite. Removal of solvents afforded the product as white solid. Yield: 94%. TLC R_f (a) 0.27; ESMS *m/z* calcd for $C_{15}H_{25}NO_4P$ $(M + H)^+$, 314.1; found, 314.2

Dodecahydro-3a,6a,9a-triaza-trindene (21′). In a round-bottom flask covered with aluminum foil, $AgNO_3$ (0.74 mmol, 126 mg) was added to a solution of pyrrolidine (0.15 mol, 10.65 g, 12.5 mL) in H_2O (140 mL) plus NaOH pellets (0.3 mol, 12 g). To this mixture, a solution of 25% $Na_2S_2O_8$ (0.15 mol, 35.7 g, 142 mL) was added dropwise at 0 °C. The reaction mixture was stirred at rt for 3 h and then extracted with DCM (2 × 200 mL), after having added NaCl to the aqueous phase to saturation. Drying over Na_2SO_4, removal of solvent, solvation in Et_2O (200 mL), filtration through neutral alumina, and evaporation to dryness afforded the product as a faint orange oil. Yield: 60%. ^{13}C NMR (50 MHz, $CDCl_3$) δ 19.9, 27.5, 45.5, 81.6.

2-Benzyl-3-(hydroxy-pyrrolidin-2-yl-phosphinoyl)-propionic Acid (26). Pd/C (10%, 1.3 g) was added to a solution of **12** (12 mmol, 5.2 g) in MeOH/H_2O (145/35 mL) and AcOH (5 drops) at 0 °C. The reaction mixture was stirred for 2 h under H_2, at rt and 1 atm, and then filtered through a pad of celite. Removal of solvents afforded the product as white solid. Yield: 95%. TLC R_f (a) 0.27; ESMS *m/z* calcd for $C_{14}H_{21}NO_4P$ $(M + H)^{-+}$, 298.1; found, 298.2.

3-{[1-(2-Acetylamino-propionyl)-pyrrolidin-2-yl]-hydroxy-phosphinoyl}-2-benzyl-propionic Acid (27). Et_3N (2 mmol, 202 mg, 0.28 mL) and BocAlaONp (1.5 mmol, 465 mg) were added to a solution of **26** (1 mmol, 0.3 g) in DMF (2 mL). The reaction mixture was stirred at rt for 12 h, concentrated in vacuo, dissolved in AcOEt (50 mL) and washed with 1 M HCl (3 × 20 mL), concentrated in vacuo, dissolved in 5% $NaHCO_3$ (50 mL) and AcOH to pH = 6–6.5, and washed with Et_2O (5 × 5 mL), acidified with 1 M HCl to pH = 1, and extracted with AcOEt (3 × 50 mL). Drying over Na_2SO_4 and evaporation of solvent afforded the protected tripeptide as white solid. Yield: 48%. Boc removal: The product (1 mmol, 468 mg) was dissolved in DCM (3 mL), TFA (3 mL) was added, and the reaction mixture was stirred at rt for 1 h and then evaporated to dryness. Acetylation: The reaction mixture was dissolved in pyridine (10 mL) and Ac_2O (3 mmol, 306 mg, 283 mL) was added and stirred at rt for 12 h. Dilution with H_2O and acidification with 1 M HCl to pH = 1, extraction with AcOEt (2 × 40 mL), drying over Na_2SO_4, evaporation of solvents, and trituration with Et_2O afforded the product as white solid. Overall yield (3 steps): 74%. HPLC (gradient 1 t = 0, 0% B; t = 10, 10% B; t = 45, 60% B; t = 50, 100% B) t_R = 21.62, 21.94, 22.48 min; (gradient 2, t = 0, 0% B; t = 10, 15% B; t = 40, 15% B; t = 45, 100% B) t_R = 19.29, 19.81, 20.53 min; ESMS *m/z* calcd for $C_{19}H_{27}N_2O_6P$ $(M - H)^-$, 409.2; found, 409.4.

3-{[1-(2-Acetylamino-3-methyl-butyryl)-pyrrolidin-2-yl]-hydroxy-phosphinoyl}-2-benzyl-propionic Acid (28). Same experimental procedure as for **27**, using BocLeuONp, afforded the product as white solid. Overall yield (3 steps): 45%. HPLC (gradient 1, t = 0, 0% B; t = 15, 23% B; t = 30, 23% B; t = 40, 40% B; t = 45, 100% B) t_R = 27.35, 29.33, 32.49, 33.21 min; (gradient 2, t = 0, 15% B; t = 20,15% B; t = 40, 100% B) t_R = 29.82, 30.29, 30.98 min; ESMS *m/z* calcd for $C_{22}H_{34}N_2O_6P$ $(M + H)^+$, 453.2; found, 453.1.

3-{[1-(2-Acetylamino-6-amino-hexanoyl)-pyrrolidin-2-yl]-hydroxy-phosphinoyl}-2-benzyl-propionic Acid (29). Same experimental procedure as for **27**, using CbzLys(Boc)ONp. Cbz removal: The product (1 mmol, 660 mg) was dissolved in MeOH/H_2O (20/5 mL) and AcOH (2 drops) 10% Pd/C (200 mg) was added at 0 °C. The reaction mixture was stirred for 2 h under H_2, at rt and 1 atm, and then filtered through a pad of celite. Removal of solvents, acetylation, and removal of the side-chain Boc group afforded the product as white solid. Overall yield (4 steps): 45%. HPLC (gradient 1, t = 0, 0% B; t = 20, 15% B; t = 40, 60% B; t = 50, 100% B) t_R = 21.42, 21.98, 22.81 min; (gradient 2, t = 0, 0% B; t = 10, 20% B; t = 30, 100% B) t_R = 14.38, 14.64, 14.92 min; ESMS *m/z* calcd for $C_{22}H_{35}N_3O_6P$ $(M + H)^+$, 468.2; found, 468.2.

4-Acetylamino-5-{2-[(2-carboxy-3-phenyl-propyl)-hydroxy-phosphinoyl]-pyrrolidin-1-yl}-5-oxo-pentanoic Acid (30). Same experimental procedure as for **29**, using CbzGlu(*t*-Bu)ONp afforded the product as white solid. Overall yield (4 steps): 42%. HPLC (gradient 1, t = 0, 0% B; t = 20, 15% B; t = 40, 15% B; t = 45, 100% B) t_R = 24.89, 25.47, 26.73 min; (gradient 2, t = 0, 0% B; t = 10, 25% B; t = 45, 75% B; t = 50, 100% B) t_R = 14.31, 14.53, 14.95 min; ESMS *m/z* calcd for $C_{21}H_{30}N_2O_8P$ $(M + H)^+$, 469.2; found, 469.2.

3-({1-[2-Acetylamino-3-(4-hydroxy-phenyl)-propionyl]-pyrrolidin-2-yl}-hydroxy-phosphinoyl)-2-benzyl-propionic Acid (31). Same experimental procedure as for **29**, using CbzTyr(Bu^t)ONp, afforded the product as white solid. Overall yield (4 steps): 50%. HPLC (gradient 1, t = 0, 0% B; t = 15, 20% B; t = 40, 60% B; t = 50, 100% B) t_R = 31.65, 32.48 min; (gradient 2, t = 0, 0% B; t = 10 15% B; t = 45, 60% B; t = 50, 100% B) t_R = 22.63, 23.59, 23.81 min; ESMS *m/z* calcd for $C_{25}H_{32}N_2O_7P$ $(M + H)^+$, 503.2; found, 503.2.

3-{[1-(2-Acetylamino-3-phenyl-propionyl)-pyrrolidin-2-yl]-hydroxy-phosphinoyl}-2-benzyl-propionic Acid (32). Same experimental procedure as for **27**, using BocPheONp, afforded the product as white solid. Overall yield (3 steps): 48%. HPLC (gradient 1, t = 0, 0% B; t = 10, 20% B; t = 45, 20% B; t = 50 100% B) t_R = 34.3, 37.2, 40.8, 42.02 min; (gradient 2, t = 0, 0% B; t = 10, 30% B; t = 30, 30% B; t = 35, 100% B) t_R = 20.65, 21.26, 23.01, 23.28 min; ESMS *m/z* calcd for $C_{25}H_{32}N_2O_6P$ $(M + H)^+$, 487.2; found, 487.2.

3-{[1-(2-Acetylamino-4-methyl-pentanoyl)-pyrrolidin-2-yl]-hydroxy-phosphinoyl}-2-benzyl-propionic Acid (33). Same experimental procedure as for **27**, using BocValONp, afforded the product as white solid. Overall yield (3 steps): 52%. HPLC (gradient 1, t = 0, 15% B; t = 20, 15% B; t = 40, 100% B) t_R = 24.22, 27.09, 28.37, 28.86 min; (gradient 2, t = 0, 0% B; t = 20, 15% B; t = 40, 60% B; t = 45, 100% B) t_R = 31.13, 31.44, 32.16, 32.40 min; ESMS *m/z* calcd for $C_{21}H_{30}N_2O_6P$ $(M - H)^-$, 437.2; found, 437.3.

3-({1-[2-Acetylamino-3-(1*H*-imidazol-4-yl)-propionyl]-pyrrolidin-2-yl}-hydroxy-phosphinoyl)-2-benzyl-propionic Acid (34). Same experimental procedure as for **27**, using TrtHis(Trt)ONp afforded the protected tripeptide as white solid. Yield: 40%. N-α-Trt removal: The product (1 mmol, 920 mg) was dissolved in DCM (9.5 mL), HCOOH (0.5 mL) was added, and the reaction mixture was stirred at rt for 10 min and then evaporated to dryness. Acetylation and removal of the side chain Trt group afforded the product as white solid. Overall yield (4 steps): 64%. HPLC (gradient 1, t = 0, 0% B; t = 5, 5% B; t = 20, 5% B; t = 30, 50% B; t = 40, 100% B) t_R = 29.01, 29.30, 29.49, 29.68 min; (gradient 2, t = 0, 0% B; t = 10, 10% B; t = 45, 35% B; t = 50, 100% B) t_R = 20.26, 21.10, 21.72, 22.21 min; ESMS *m/z* calcd for $C_{22}H_{28}N_4O_6P$ $(M - H)^-$, 475.2; found, 475.5.

3-{[1-(2-Acetylamino-4-methyl-pentanoylamino)-2-phenyl-ethyl]-hydroxy-phosphinoyl}-2-benzyl-propionic Acid (35). Same experimental procedure as for **33**, using the phosphinic dipeptide **19**, afforded the product as white solid. Overall yield (3 steps): 52%. HPLC (gradient 1, t = 0, 0% B; t = 10, 25% B; t = 45, 75% B; t = 50, 100% B) t_R = 31.39, 31.88, 32.86 min; (gradient 2, t = 0, 0% B; t = 10, 35% B; t = 45, 35% B; t = 50, 100% B) t_R =

22.45, 22.89, 24.34 min; ESMS *m/z* calcd for $C_{26}H_{36}N_2O_6P$ $(M + H)^+$, 503.2; found, 503.2.

3-({1-[2-Acetylamino-3-(1*H*-imidazol-4-yl)-propionylamino]-3-methyl-butyl}-hydroxy-phosphinoyl)-2-benzyl-propionic Acid (36). Same experimental procedure as for **34**, using the phosphinic dipeptide **20**, afforded the product as white solid. Overall yield (3 steps): 42%. HPLC (gradient 1, $t = 0$, 0% B; $t = 20$, 15% B; $t = 40$, 60% B; $t = 50$, 100% B) $t_R = 28.80$, 29.90, 30.85, 31.70 min; (gradient 2, $t = 0$, 0% B; $t = 10$, 25% B, $t = 45$, 75% B; $t = 50$, 100% B) $t_R = 15.65$, 16.27, 16.96, 17.86 min; ESMS *m/z* calcd for $C_{23}H_{34}N_4O_6P$ $(M + H)^+$, 493.2; found, 493.2.

2-Hydroxyphosphinoylmethyl-pent-4-ynoic Acid Ethyl Ester (37). Ammonium hypophosphate salt $H_2P(O)(O^-NH_4^+)$ is produced by mixing equimolecular quantities of commercially available aqueous solutions of 50% H_3PO_2 and 25% NH_3 at 0 °C, evaporation of water, and drying over P_2O_5 to constant weight. A suspension of dry $H_2P(O)(O^-NH_4^+)$ (0.17 mol, 14.11 g) and HMDS (0.17 mol, 27.41 g, 35 mL) was heated at 110 °C for 3 h under argon atmosphere. The reaction mixture was then cooled to rt, 200 mL of dry DCM was added, and after cooling, to 0 °C, $CH_2{=}C(CH_2C{\equiv}CH)COOEt$ (34 mmol, 4.69 g) in DCM (35 mL) was added at this temperature dropwise for 15 min and the reaction mixture was stirred for 12 h at rt. Then absolute EtOH (35 mL) was added dropwise. The reaction mixture was evaporated in vacuo, then dissolved in 5% $NaHCO_3$ (200 mL), washed with Et_2O (2 × 100 mL), acidified with 6 M HCl to pH = 1, and extracted with AcOEt (3 × 150 mL), dried over Na_2SO_4, and evaporation to dryness afforded the product as viscous colorless oil. Yield: 88%. TLC R_f ($CHCl_3$/MeOH/AcOH = 7/2/1) 0.59. ^{1}H NMR (200 MHz, $CDCl_3$) δ 1.28 (t, $J = 7.2$ Hz, 3H), 1.98–2.4 (m, 3H), 2.63–2.66 (m, 2H), 4.20 (q, $J = 7.2$ Hz, 2H), 7.27 (d, $J = 568.37$ Hz, 1H); ^{13}C NMR (50 MHz, $CDCl_3$) δ 14.31, 22.19 (d, $^3J_{PC} = 12.03$ Hz) 29.9 (d, $^1J_{PC} = 97.57$ Hz), 37.91 (d, $^1J_{PC} = 98.9$ Hz), 61.54, 71.32, 79.66, 172.27; ^{31}P NMR (81 MHz, $CDCl_3$) δ 34.62; ESMS *m/z* calcd for $C_8H_{12}O_4P$ $(M - H)^-$, 203.1; found, 203.2.

2-[(2-Ethoxycarbonyl-pent-4-ynyl)-hydroxy-phosphinoyl]-pyrrolidine-1-carboxylic Acid Benzyl Ester (38). Same procedure as for **3** (method b), starting from **37**. Yield: 54%. TLC R_f ($CHCl_3$/MeOH/AcOH = 7/0.5/0.5) 0.59. ^{1}H NMR (200 MHz, $CDCl_3$) δ 1.16–1.34 (m, 3H), 1.79–2.70 (m, 9H), 2.84–3.10 (m, 1H), 3.38–3.68 (m, 2H), 4.02–4.27 (m, 3H), 5.05–5.20 (m, 2H), 7.22–7.41 (m, 5H); ^{13}C NMR (50 MHz, $CDCl_3$) δ 14.09, 22.34, 23.45, 24.65, 25.37, 26.05, 28.53 (d, $^1J_{PC} = 94.57$ Hz), 38.04, 47.18, 56.05 (d, $^1J_{PC} = 108.33$ Hz), 56.46 (d, $^1J_{PC} = 108.33$ Hz), 60.97, 67.39, 70.74, 80.09, 127.79, 128.05, 128.44, 136.20, 155.69, 172.93; ^{31}P NMR (81 MHz, $CDCl_3$) δ 55.84, 55.70, 55.42; ESMS *m/z* calcd for $C_{20}H_{25}NO_6P$ $(M - H)^-$, 406.2; found, 406.3.

2-{[2-Ethoxycarbonyl-3-(3-phenyl-isoxazol-5-yl)-propyl]-hydroxy-phosphinoyl}-pyrrolidine-1-carboxylic Acid Benzyl Ester (39). NCS (1.27 mmol, 170 mg) and pyridine (0.94 mmol, 74 mg, 76 μL) were added to a solution of benzaldehyde oxime (1.27 mmol, 154 mg) in $CHCl_3$ (7 mL). The reaction mixture was stirred at 45 °C for 3 h and then **38** (0.42 mmol, 160 mg) dissolved in $CHCl_3$ (250 μL) and Et_3N (1.68 mmol, 170 mg, 232 μL) were added in five portions. The reaction mixture was stirred at 45 °C for 3 days. Removal of solvents, solvation in $NaHCO_3$ 5% (50 mL), washings with Et_2O (3 × 5 mL), acidified with 2 M HCl to pH = 1, and extracted with AcOEt (3 × 30 mL), dried over Na_2SO_4, and evaporation to dryness afforded the crude product. The reaction was repeated three times until consumption of **38**, as shown by ^{31}P NMR. Purification by column chromatography, using $CHCl_3$/MeOH/AcOH (7/0.3/0.3) as eluent, afforded the product as oyster-white foam. Yield: 80%. TLC R_f ($CHCl_3$/MeOH/AcOH = 7/0.5/0.5) 0.59. HPLC (gradient $t = 0$, 0% B; $t = 10$, 25% B; $t = 45$, 75% B; $t = 50$, 100% B) $t_R = 38.71$, 38.98 min; ^{1}H NMR (200 MHz, $CDCl_3$) δ 1.00–1.32 (m, 3H), 1.72–2.53 (m, 6H), 3.01–3.69 (m, 5H), 4.00–4.25 (m, 3H), 6.26–6.49 (m, 1H), 7.16–7.85 (m, 10H); ^{13}C NMR (50 MHz, $CDCl_3$) δ 13.9, 24.66, 25.43, 28.45, 30.04, 37.83, 47.16, 56.06 (d, $^1J_{PC} = 110.78$ Hz), 56.59 (d, $^1J_{PC} = 110.78$ Hz), 61.16, 67.53, 100.52, 126.67, 127.81, 128.10, 128.46, 128.78, 129.81, 136.09, 155.76, 162.31, 170.12, 172.97; ^{31}P NMR (81 MHz, $CDCl_3$) δ 55.17; ESMS *m/z* calcd for $C_{27}H_{29}N_2O_7P$ $(M - H)^-$, 525.2; found, 525.3.

3-{[1-(2-Acetylamino-4-methyl-pentanoyl)-pyrrolidin-2-yl]-hydroxy-phosphinoyl}-2-(3-phenyl-isoxazol-5-ylmethyl)-propionic Acid (40). Same procedure as described for **33**, using the hydrogenated derivative of phosphinic dipeptide **39**, afforded the product as white solid. Overall yield (3 steps): 51%. HPLC (gradient 1, $t = 0$, 0% B; $t = 10$, 25% B; $t = 45$, 75% B; $t = 50$, 100% B) $t_R = 22.67$, 22.98, 25.15 min; (gradient 2, $t = 0$, 0% B; $t = 15$, 25% B; $t = 30$, 25% B; $t = 40$, 45% B; $t = 50$, 100% B) $t_R = 35.82$, 37.31, 41.50 min; ESMS *m/z* calcd for $C_{25}H_{33}N_3O_7P$ $(M - H)^-$, 518.2; found, 518.3.

3-({1-[2-Acetylamino-3-(1*H*-imidazol-4-yl)-propionyl]-pyrrolidin-2-yl}-hydroxy-phosphinoyl)-2-(3-phenyl-isoxazol-5-ylmethyl)-propionic Acid (41). Same procedure as described for **34**, using the hydrogenated derivative of phosphinic dipeptide **39**, afforded the product as white solid. Overall yield (4 steps): 42%. HPLC (gradient 1, $t = 0$, 0% B; $t = 20$, 15% B; $t = 40$, 60% B; $t = 45$, 100% B) $t_R = 28.09$, 28.67, 29.29, 29.88 min; (gradient 2, $t = 0$, 0% B; $t = 10$, 10% B; $t = 20$, 10% B; $t = 30$, 100% B) $t_R = 27.49$, 28.04 min; ESMS *m/z* calcd for $C_{25}H_{31}N_5O_7P$ $(M + H)^+$, 544.2; found, 544.1.

2-[(1-Benzyloxycarbonylamino-3-methyl-butyl)-hydroxy-phosphinoylmethyl]-pent-4-ynoic Acid Ethyl Ester (42). Same experimental procedure as for **3**, method A, using **7** and $CH_2{=}C(CH_2C{\equiv}CH)COOEt$ product afforded as white solid. Yield 98%. TLC R_f ($CHCl_3$/MeOH/AcOH = 7/0.5/0.5) 0.59. ^{1}H NMR (200 MHz, DMSO-d_6) δ 0.63–0.97 (m, 6H), 1.02–1.28 (m, 3H), 1.31–2.13 (m, 5H), 2.69–2.94 (m, 2H), 3.61–3.86 (m, 1H), 3.92–4.19 (m, 2H), 4.88–5.19 (m, 2H), 7.20–7.42 (m, 5H); ^{13}C NMR (50 MHz, $CDCl_3$) δ 14.03, 20.98, 22.26, 23.36, 24.27, 26.75 (d, $^1J_{PC} = 91.78$ Hz), 36.10, 37.89, 47.92 (d, $^1J_{PC} = 105.56$ Hz), 48.46 (d, $^1J_{PC} = 105.56$ Hz), 61.18, 67.05, 71.00, 79.94, 127.85, 128.03, 128.40, 136.24, 156.09, 172.82; ^{31}P NMR (81 MHz, DMSO-d_6) δ 46.23, 46.44; ESMS *m/z* calcd for $C_{21}H_{31}NO_6P$ $(M + H)^+$, 424.2; found, 424.3.

3-[(1-Benzyloxycarbonylamino-3-methyl-butyl)-hydroxy-phosphinoyl]-2-(3-phenyl-isoxazol-5-ylmethyl)-propionic Acid Ethyl Ester (43). Same experimental procedure as described for **41**, using the phosphinic dipeptide **39**, afforded the product as white solid. Yield: 83%. HPLC (gradient, $t = 0$, 0% B; $t = 10$, 35% B; $t = 35$, 100% B) $t_R = 29.54$ min. ^{1}H NMR (200 MHz, $CDCl_3$) δ 0.82–0.96 (m, 6H), 1.09–1.28 (m, 3H), 1.45–1.77 (m, 5H), 1.81–2.04 (m, 1H), 2.14–2.38 (m, 1H), 3.07–3.35 (m, 3H), 4.00–4.20 (m, 3H), 5.05–5.11 (m, 2H), 6.34–6.38 (m, 1H), 7.24–7.45 (m, 10H); ^{13}C NMR (50 MHz, $CDCl_3$) δ 13.96, 20.91, 23.32, 24.31, 26.75, 28.25, 28.54, 29.64, 29.82, 30.02, 30.23, 35.95, 37.85, 47.96 (d, $^1J_{PC} = 106.25$ Hz), 48.61 (d, $^1J_{PC} = 106.25$ Hz), 61.48, 67.20, 100.68, 126.05, 126.71, 127.87, 127.94, 128.14, 128.45, 128.83, 129.92, 136.16, 156.29, 162.28, 169.96, 173.05; ^{31}P NMR (81 MHz, d_6 $CDCl_3$) δ 53.62; ESMS *m/z* calcd for $C_{28}H_{36}N_2O_7P$ $(M + H)^+$, 543.2; found, 543.2.

3-({1-[2-Acetylamino-3-(1*H*-imidazol-4-yl)-propionylamino]-3-methyl-butyl}-hydroxy-phosphinoyl)-2-(3-phenyl-isoxazol-5-ylmethyl)-propionic Acid (44). Same experimental procedure as described for **41**, using the hydrogenated derivative of phosphinic dipeptide **43**, afforded the product as white solid. Overall yield (4 steps): 49%. HPLC (gradient 1, $t = 0$, 0% B; $t = 45$, 100% B) $t_R = 19.11$, 19.41, 20.08, 20.54 min; (gradient 2, $t = 0$, 0% B; $t = 20$, 20% B; $t = 40$, 60% B; $t = 50$, 100% B) $t_R = 31.40$, 31.80, 32.47, 33.03 min; ESMS *m/z* calcd for $C_{26}H_{35}N_5O_7P$ $(M + H)^+$, 560.2; found, 560.3.

Inhibitor Potency

ACE2. K_i values reported in Table 1 were determined using, respectively, ACE2 (0.3 nM final from R&D systems) and Mca-APK(Dnp) as substrate (35 μM final) from R&D systems. Enzyme and inhibitors were incubated for 45 min before the initiation of the reaction by substrate addition. Assays were carried out at 25 °C in 50 mM Hepes (pH 6.8), 1 M NaCl, 10

μM $ZnCl_2$. Continuous assays were performed by recording the fluorescence increase at 405 nm ($\epsilon_{ex} = 320$ nm) induced by the cleavage of Mca-APK(Dnp)OH by ACE2, using black, flat-bottomed, 96-well nonbinding surface plates (Corning-Costar, Schiphol-RijK, The Netherlands). Fluorescence signals were monitored using a Fluoroscan Ascent photon counter spectrophotometer (Thermo-Labsystems, Courtaboeuf, France) equipped with a temperature control device and a plate shaker. The substrate and enzyme concentrations for the experiments were chosen so as to remain well below 10% of substrate utilization and to observe initial rates. For each inhibitor, percentage inhibition was determined in triplicate experiments at five inhibitor concentrations, chosen to observe a 20–80% range of inhibition. K_i values were determined using the method proposed by Horovitz and Leviski.[35]

ACE. Assays were performed as described for ACE2, using Mca-Ala-Ser-Asp-Lys-Dpa-OH, as substrate (15 μM) and somatic ACE (0.5 nM) from R&D systems.

CPA. inhibitor potencies toward bovine carboxypeptidase A (Sigma-Aldrich Co) were determined, as described previously.[18] Inhibitors were added to 0.5 nM bovine pancreatic CPA (Sigma-Aldrich) in assay buffer (50 mM Tris-HCl, 1 M NaCl, pH 7.5). Furylacryloyl-Phe-Phe substrate (50 μM) was added to start the reaction. Activity was monitored by measuring decrease in absorbance (328 nm).

Molecular Modeling

The molecular model of the interaction of compound **40** with ACE2, based on the crystal structure of ACE2 in interaction with MLN-4760 (PDB code 1R4L), was achieved with program CHARMM (version 27), using version 22. The geometrical and nonbonded parameters for compound **40** were derived from ab initio quantum calculations with the program Gaussian98. These calculations were done at the MP2 level of theory using a 6-31+G(d,p) basis set. An initial model of compound **40** was built with the Insight software (Accelrys Inc.). The initial position of compound **40** in the ACE2 active site was obtained by superimposition of the main chain atoms of compound **40** on the corresponding atoms of the phosphinic peptide RXPA380, as observed in the crystal structure of this inhibitor with the germinal form of ACE (PDB code 2oc2). This starting structure was then refined by energy minimization and molecular dynamics with CHARMM. To preserve the structure of the protein during relaxation of the complex, harmonic restraints were applied to the atomic positions of several sets of atoms. The harmonic constants were set to 100, 5, and 0.5 $kcal^{-1}$ $Å^{-2}$ for the ions and their chelating residues, the atoms and the residues of the protein located at a distance greater than 5 Å, respectively. The initial step of the relaxation protocol consists of an initial 2000 cycles of adopted basis Newton–Raphson energy minimization. Then 100000 steps of molecular dynamics using the Verlet algorithm were undertaken. The integration step was set to 0.0005 ps. The temperature was gradually increased by 25 K each 1000 steps to reach 300 K. This molecular dynamics run was followed by 5000 cycles of energy minimization. The resulting structure was then analyzed. During the calculations, the nonbonded interactions were modeled using a Lennard−Jones function and a Coulombic electrostatic term with a nonbonded cutoff of 13 Å. The dielectric constant was set to 1.

Acknowledgment. This work was supported by funds from Commissariat à l'Energie Atomique and from the Laboratory of Organic Chemistry, Special Account for research Grants of NKUA and Pythagoras II (EPEAK II).

Supporting Information Available: ^1H, ^{13}C, and ^{31}P NMR spectra of compounds **3–5**, **9–11**, **37–39**, **42**, and **43** and HPLC chromatograms of compounds **27–36**, **40**, **41**, and **44**. This material is available free of charge via the Internet at http://pubs.acs.org.

References

(1) Erdos, E. G. Angiotensin I converting enzyme and the changes in our concepts through the years. Lewis K. Dahl memorial lecture. *Hypertension* **1990**, *16*, 363–70.
(2) Barllo, M.; Jiao, X. Y.; Wojtowicz, H.; Rajan, P.; Verbuggen, C.; Augustyns, K.; Haemers, A. Convenient one-pot preparation of disubstituted phosphinic acids derived from simple amino acids and proline. *Synthesis* **1995**, 1074–75.
(3) Zaman, M. A.; Oparil, S.; Calhoun, D. A. Drugs targeting the renin-angiotensin-aldosterone system. *Nat. Rev. Drug Discovery* **2002**, *1*, 621–36.
(4) Wong, J.; Patel, R. A.; Kowey, P. R. The clinical use of angiotensin-converting enzyme inhibitors. *Prog. Cardiovasc. Dis.* **2004**, *47*, 116–30.
(5) Tipnis, S. R.; Hooper, N. M.; Hyde, R.; Karran, E.; Christie, G.; Turner, A. J. A human homolog of angiotensin-converting enzyme. Cloning and functional expression as a captopril-insensitive carboxypeptidase. *J. Biol. Chem.* **2000**, *275*, 33238–43.
(6) Donoghue, M.; Hsieh, F.; Baronas, E.; Godbout, K.; Gosselin, M.; Stagliano, N.; Donovan, M.; Woolf, B.; Robison, K.; Jeyaseelan, R.; Breitbart, R. E.; Acton, S. A novel angiotensin-converting enzyme-related carboxypeptidase (ACE2) converts angiotensin I to angiotensin 1–9. *Circ. Res.* **2000**, *87*, E1–9.
(7) Vickers, C.; Hales, P.; Kaushik, V.; Dick, L.; Gavin, J.; Tang, J.; Godbout, K.; Parsons, T.; Baronas, E.; Hsieh, F.; Acton, S.; Patane, M.; Nichols, A.; Tummino, P. Hydrolysis of biological peptides by human angiotensin-converting enzyme-related carboxypeptidase. *J. Biol. Chem.* **2002**, *277*, 14838–43.
(8) Brosnihan, K. B.; Neves, L. A.; Chappell, M. C. Does the angiotensin-converting enzyme (ACE)/ACE2 balance contribute to the fate of angiotensin peptides in programmed hypertension. *Hypertension* **2005**, *46*, 1097–9.
(9) Der Sarkissian, S.; Huentelman, M. J.; Stewart, J.; Katovich, M. J.; Raizada, M. K. ACE2: A novel therapeutic target for cardiovascular diseases. *Prog. Biophys. Mol. Biol.* **2006**, *91*, 163–98.
(10) Oudit, G. Y.; Crackower, M. A.; Backx, P. H.; Penninger, J. M. The role of ACE2 in cardiovascular physiology. *Trends Cardiovasc. Med.* **2003**, *13*, 93–101.
(11) Hamming, I.; Cooper, M. E.; Haagmans, B. L.; Hooper, N. M.; Korstanje, R.; Osterhaus, A. D.; Timens, W.; Turner, A. J.; Navis, G.; van Goor, H. The emerging role of ACE2 in physiology and disease. *J. Pathol.* **2007**, *212*, 1–11.
(12) Crackower, M. A.; Sarao, R.; Oudit, G. Y.; Yagil, C.; Kozieradzki, I.; Scanga, S. E.; Oliveira-dos-Santos, A. J.; da Costa, J.; Zhang, L.; Pei, Y.; Scholey, J.; Ferrario, C. M.; Manoukian, A. S.; Chappell, M. C.; Backx, P. H.; Yagil, Y.; Penninger, J. M. Angiotensin-converting enzyme 2 is an essential regulator of heart function. *Nature* **2002**, *417*, 822–8.
(13) Gurley, S. B.; Allred, A.; Le, T. H.; Griffiths, R.; Mao, L.; Philip, N.; Haystead, T. A.; Donoghue, M.; Breitbart, R. E.; Acton, S. L.; Rockman, H. A.; Coffman, T. M. Altered blood pressure responses and normal cardiac phenotype in ACE2-null mice. *J. Clin. Invest.* **2006**, *116*, 2218–25.
(14) Ashley, E.; Chun, H. J.; Quertermous, T. Opposing cardiovascular roles for the angiotensin and apelin signaling pathways. *J. Mol. Cell. Cardiol.* **2006**, *41*, 778–81.
(15) Ishida, J.; Hashimoto, T.; Hashimoto, Y.; Nishiwaki, S.; Iguchi, T.; Harada, S.; Sugaya, T.; Matsuzaki, H.; Yamamoto, R.; Shiota, N.; Okunishi, H.; Kihara, M.; Umemura, S.; Sugiyama, F.; Yagami, K.; Kasuya, Y.; Mochizuki, N.; Fukamizu, A. Regulatory roles for APJ, a seven-transmembrane receptor related to angiotensin-type 1 receptor in blood pressure in vivo. *J. Biol. Chem.* **2004**, *279*, 26274–9.
(16) Lee, D. K.; George, S. R.; O'Dowd, B. F. Unravelling the roles of the apelin system: prospective therapeutic applications in heart failure and obesity. *Trends Pharmacol. Sci.* **2006**, *27*, 190–4.
(17) El Messari, S.; Iturrioz, X.; Fassot, C.; De Mota, N.; Roesch, D.; Llorens-Cortes, C. Functional dissociation of apelin receptor signaling and endocytosis: implications for the effects of apelin on arterial blood pressure. *J. Neurochem.* **2004**, *90*, 1290–301.
(18) Dales, N. A.; Gould, A. E.; Brown, J. A.; Calderwood, E. F.; Guan, B.; Minor, C. A.; Gavin, J. M.; Hales, P.; Kaushik, V. K.; Stewart, M.; Tummino, P. J.; Vickers, C. S.; Ocain, T. D.; Patane, M. A. Substrate-based design of the first class of angiotensin-converting enzyme-related carboxypeptidase (ACE2) inhibitors. *J. Am. Chem. Soc.* **2002**, *124*, 11852–3.

(19) Towler, P.; Staker, B.; Prasad, S. G.; Menon, S.; Tang, J.; Parsons, T.; Ryan, D.; Fisher, M.; Williams, D.; Dales, N. A.; Patane, M. A.; Pantoliano, M. W. ACE2 X-ray structures reveal a large hinge-bending motion important for inhibitor binding and catalysis. *J. Biol. Chem.* **2004**, *279*, 17996–8007.

(20) Ye, M.; Wysocki, J.; William, J.; Soler, M. J.; Cokic, I.; Batlle, D. Glomerular localization and expression of angiotensin-converting enzyme 2 and angiotensin-converting enzyme: Implications for albuminuria in diabetes. *J. Am. Soc. Nephrol.* **2006**, *17*, 3067–75.

(21) Georgiadis, D.; Beau, F.; Czarny, B.; Cotton, J.; Yiotakis, A.; Dive, V. Roles of the two active sites of somatic angiotensin-converting enzyme in the cleavage of angiotensin I and bradykinin: insights from selective inhibitors. *Circ. Res.* **2003**, *93*, 148–54.

(22) Dive, V.; Georgiadis, D.; Matziari, M.; Makaritis, A.; Beau, F.; Cuniasse, P.; Yiotakis, A. Phosphinic peptides as zinc metalloproteinase inhibitors. *Cell. Mol. Life Sci.* **2004**, *61*, 2010–9.

(23) Dive, V.; Andarawewa, K. L.; Boulay, A.; Matziari, M.; Beau, F.; Guerin, E.; Rousseau, B.; Yiotakis, A.; Rio, M. C. Dosing and scheduling influence the antitumor efficacy of a phosphinic peptide inhibitor of matrix metalloproteinases. *Int. J. Cancer* **2005**, *113*, 775–81.

(24) Grams, F.; Dive, V.; Yiotakis, A.; Yiallouros, I.; Vassiliou, S.; Zwilling, R.; Bode, W.; Stocker, W. Structure of astacin with a transition-state analogue inhibitor. *Nat. Struct. Biol.* **1996**, *3*, 671–5.

(25) Gall, A. L.; Ruff, M.; Kannan, R.; Cuniasse, P.; Yiotakis, A.; Dive, V.; Rio, M. C.; Basset, P.; Moras, D. Crystal structure of the stromelysin-3 (MMP-11) catalytic domain complexed with a phosphinic inhibitor mimicking the transition-state. *J. Mol. Biol.* **2001**, *307*, 577–86.

(26) Corradi, H. R.; Chitapi, I.; Sewell, B. T.; Georgiadis, D.; Dive, V.; Sturrock, E. D.; Acharya, K. R. The structure of testis angiotensin-converting enzyme in complex with the C domain-specific inhibitor RXPA380. *Biochemistry* **2007**, *46*, 5473–8.

(27) Tochowicz, A.; Maskos, K.; Huber, R.; Oltenfreiter, R.; Dive, V.; Yiotakis, A.; Zanda, M.; Bode, W.; Goettig, P. Crystal structures of MMP-9 complexes with five inhibitors: contribution of the flexible Arg424 side-chain to selectivity. *J. Mol. Biol.* **2007**, *371*, 989–1006.

(28) Rella, M.; Rushworth, C. A.; Guy, J. L.; Turner, A. J.; Langer, T.; Jackson, R. M. Structure-based pharmacophore design and virtual screening for novel angiotensin converting enzyme 2 inhibitors. *J. Chem. Inf. Model.* **2006**, *46*, 708–16.

(29) Huentelman, M. J.; Zubcevic, J.; Hernandez Prada, J. A.; Xiao, X.; Dimitrov, D. S.; Raizada, M. K.; Ostrov, D. A. Structure-based discovery of a novel angiotensin-converting enzyme 2 inhibitor. *Hypertension* **2004**, *44*, 903–6.

(30) Huang, L.; Sexton, D. J.; Skogerson, K.; Devlin, M.; Smith, R.; Sanyal, I.; Parry, T.; Kent, R.; Enright, J.; Wu, Q. L.; Conley, G.; DeOliveira, D.; Morganelli, L.; Ducar, M.; Wescott, C. R.; Ladner, R. C. Novel peptide inhibitors of angiotensin-converting enzyme 2. *J. Biol. Chem.* **2003**, *278*, 15532–40.

(31) Yiotakis, A.; Vassiliou, S.; Jiracek, J.; Dive, V. Protection of the hydroxyphosphinyl function of phosphinic dipeptides by adamantyl. Application to the solid-phase synthesis of phosphinic peptides. *J. Org. Chem.* **1996**, *61*, 6601–6605.

(32) Baylis, E. K.; Cambell, M.; Dingwall, J. G. 1-aminoalkylphosphonous acids. part 1. isosteres of the protein aminoacids. *J. Chem. Soc., Perkin. Trans. 1* **1984**, 2845–853.

(33) Stetter, H.; Kuhlman, H. Eine einfache Herstellung von α-alkyl-acrysäure-ester. *Synthesis* **1979**, 20–30.

(34) Nomura, Y.; Ogawa, K.; Takeuchi, Y.; Tomoda, S. One-step synthesis and structural confirmation of 1-pyrroline trimer. *Chem. Lett.* **1977**, 693–96.

(35) Horovitz, A.; Levitzki, A. An accurate method for determination of receptor-ligand and enzyme-inhibitor dissociation constants from displacement curves. *Proc. Natl. Acad. Sci. U.S.A.* **1987**, *84*, 6654–8.

JM701275Z